Resonance strength for *KLL* dielectronic recombination of hydrogenlike krypton

Zhimin Hu,[1,2,*] Yueming Li,[3] and Nobuyuki Nakamura[1]

[1]*Institute for Laser Science, The University of Electro-communications, Chofu, Tokyo 182-8585, Japan*

[2]*Research Center of Laser Fusion, P. O. Box 919-986, Mianyang 621900, China*

[3]*Institute of Applied Physics and Computational Mathematics, P. O. Box 8009, Beijing 100088, China*

(Received 4 April 2013; published 16 May 2013)

We report *KLL* dielectronic recombination (DR) resonance strength for hydrogenlike krypton Kr^{35+} measured with an electron-beam ion trap. X rays emitted from both DR and radiative recombination (RR) are observed as a function of electron-beam energy over the *KLL* resonances. The DR resonance strength is obtained by normalizing the DR x-ray counts to theoretical RR cross sections. The experimental strength is shown to agree with theoretical strength calculated using the flexible atomic code.

DOI: 10.1103/PhysRevA.87.052706 PACS number(s): 34.80.Lx

I. INTRODUCTION

Dielectronic recombination (DR) plays an important role in hot plasmas, because it strongly affects the ionization dynamics [1,2]. DR is a two-step process composed of resonant electron capture which results in a doubly excited state and radiative decay of the doubly excited state. For example, it can be written for hydrogenlike ions as follows:

$$\begin{aligned} e + \mathrm{A}^{q+}(1s) &\rightarrow \mathrm{A}^{(q-1)+**}(2l2l') \\ &\rightarrow \mathrm{A}^{(q-1)+*}(1s2l') + h\nu_1 \\ &\rightarrow \mathrm{A}^{(q-1)+}(1s^2) + h\nu_1 + h\nu_2. \end{aligned}$$

The process is also schematically shown in Fig. 1. In this process (which is referred to as the *KLL* DR as a K-shell electron is excited to the L shell with capturing a free electron to the L shell), a K-shell vacancy is still left after the primary x-ray decay of the doubly excited state. Thus the singly excited state can also decay by emitting another K x ray, whose energy is slightly different from that of the primary one.

An electron-beam ion trap (EBIT) [3,4] is a suitable device for studying DR. It can trap highly charged ions interacting with a quasimonoenergetic electron beam. DR processes can be studied by observing DR x rays with scanning the electron energy. To date, DR processes have been studied extensively for heliumlike or lower charged ions [5–14]. On the other hand, DR of hydrogenlike ions has been studied only for a few ions [15–17] because large switching of electron energy is needed between "cooking" and probing energies ("cooking" energy refers to the electron energy for producing the ions).

In this paper, we present DR measurement of hydrogenlike krypton ions with the Tokyo EBIT [18]. DR resonance strengths are obtained by normalizing the DR x-ray intensities to theoretical radiative recombination (RR) cross sections. Experimentally obtained strengths are compared with theoretical values calculated by using the flexible atomic code [19].

II. EXPERIMENT

The experimental method is practically the same as that used in our previous studies [15,16] and will be briefly described here. In the present experiment, krypton gas was introduced continually into the trapping region of the Tokyo EBIT [18]. The electron-beam energy was fixed for 2 s at 28 keV, which is enough higher than the ionization energy of heliumlike krypton (17.3 keV). After this cooking time, the electron energy was scanned between 8 and 10 keV for probing the *KLL* DR resonances. This probing time was about 10 ms, and then the energy was switched back to the cooking energy and kept for 90 ms to preserve the hydrogenlike ion abundance. During each probing period, the energy scan was repeated five cycles, as shown in Fig. 2. The trapped ions were dumped every 10 s to avoid the accumulation of unwanted ions, such as barium and tungsten ions, in the trapping region. X rays emitted from the trapped ions were detected with a high purity Ge detector placed at 90° with respect to the electron-beam propagation direction. The EBIT operation parameters of the present experiment are summarized in Table I. The parameters other than the electron energy were fixed throughout the measurement.

The pulse height (corresponding to the x-ray energy) of each signal from the Ge detector was recorded with the beam energy at the time when the signal was detected. Figure 3 shows two-dimensional x-ray intensity distribution as functions of x-ray energy and electron energy. The bright spots in the figure correspond to the x-ray intensity enhancement due to DR resonances.

III. THEORETICAL CALCULATIONS

For analysis and comparison, resonance strengths were calculated with the flexible atomic code (FAC), which was developed by Gu [19] based on the relativistic configuration-interaction method. The results for 15 dominant *KLL* resonant states are listed in Table II with the resonant energy E_r and the dielectronic-capture resonance strength S_{DC}. The doubly excited states produced by dielectronic capture can decay to a singly excited $1s2l$ state with emitting a K x-ray photon. The x-ray emission generally has an anisotropic angular distribution because the ions are excited by the impact of an unidirectional electron beam in an EBIT [20–24]. For the comparison with the experiment at an observation angle of 90°, the angular distribution was also calculated using the FAC code. The angular distribution correction coefficient [24]

*zhimin.hu@yahoo.com; Present address: Research Center of Laser Fusion, P. O. Box 919-986, Mianyang 621900, China.

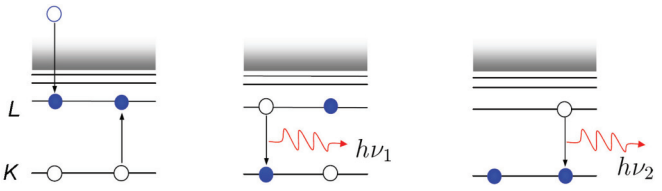

FIG. 1. (Color online) Schematic illustration of the *KLL* DR process into a hydrogenlike ion.

at $\theta = 90^\circ$ can be expressed as [25]:

$$W(90^\circ) = 1 - \tfrac{1}{2}\alpha\mathcal{A}, \tag{1}$$

where α is the intrinsic anisotropy parameter which is determined by the angular momentum of the initial (J_i) and final (J_f) states of the transition, and $\mathcal{A}$ is the alignment parameter of the initial state [26,27]. For the electric dipole ($E1$) transitions, the intrinsic angular distribution coefficient α can be expressed as [28]

$$\alpha(J_i, J_f) = 3\sqrt{5}(-1)^{J_i+J_f-1}(2J_i+1)^{1/2} \times \begin{pmatrix} 1 & 1 & 2 \\ 1 & -1 & 0 \end{pmatrix} \begin{Bmatrix} 1 & 1 & 2 \\ J_i & J_i & J_f \end{Bmatrix}, \tag{2}$$

where the quantity in large parentheses and braces denote the Wigner $3j$ and $6j$ symbols, respectively. It should be noted that $W(90^\circ)$ is unity (corresponding to the uniform distribution) for the transitions with a $J = 0$ upper state because only one magnetic sublevel with $M_J = 0$ is possible. Table II also lists theoretical differential strengths for the first K x-ray emission ($dS^{1st}/d\Omega$), which were calculated from S_{DC}, $W(90^\circ)$, and the branching ratio (BR).

Almost all the singly excited $1s2l$ states produced via the first K x-ray emission decay to the ground state $1s^2$ with emitting a second K x-ray photon. In order to calculate the angular distribution $W(90^\circ)$ of the second decay, the alignment parameter $\mathcal{A}_s$ for singly excited $1s2l$ states was calculated by [28,29]

$$\mathcal{A}_s = \mathcal{A}_d U(J_s, J_d), \tag{3}$$

where $\mathcal{A}_d$ is the alignment parameter for the doubly excited resonant state, $U(J_s, J_d)$ the deorientation factor of the transition $J_s \rightarrow J_d$, and J_d, J_s the total angular momentum of the intermediate doubly excited and singly excited states,

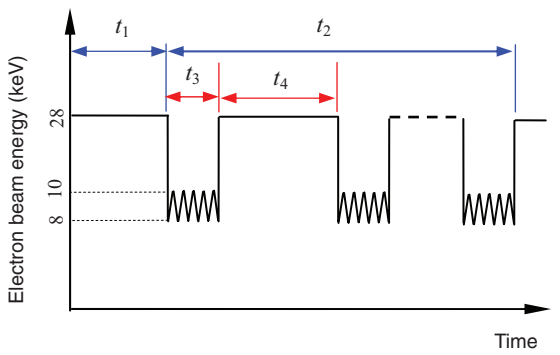

FIG. 2. (Color online) Time sequence for the electron-beam energy scan. In the present experiment, t_1, t_2, t_3, and t_4 was 2 s, 8 s, 10 ms, and 90 ms, respectively.

TABLE I. Operational parameters of the Tokyo electron-beam ion trap in the present experiment.

Parameter	Value
Electron beam current	40 mA
Magnetic field	3 T
Trap potential	50 V
Scan energy	8–10 keV
Sweep rate	2 eV/μs
Dumping period	10 s
Pressure of gas injector	2×10^{-5} Pa

respectively. Consequently, the differential strengths for the second K x-ray emission ($dS^{2nd}/d\Omega$) were obtained as listed in Table II.

For the decay of the singly excited $1s2l$ states, we must consider two exceptional cases where the direct decay to $1s^2$ is not available; one is $[1s2s]_0$ which decays via two photon emission with a branching ratio of unity, and another is $[1s2p_{3/2}]_2$ which can decay to $[1s2s]_1$ with a theoretical branching ratio of 0.103. For the former, the differential strength $dS^{2nd}/d\Omega$ should be zero because only the process involving K x-ray emission is of the present interest. For the latter, $W(90^\circ)$ should be calculated by taking the deorientation from $\mathcal{A}([1s2p_{3/2}]_2)$ to $\mathcal{A}([1s2s]_1)$. The finally obtained differential strengths $dS^{2nd}/d\Omega$ are given in Table II.

For including the contributions from lower charge state ions in the analysis, the differential resonance strengths of heliumlike and lithiumlike krypton were also calculated and listed in Tables III and IV. In addition, the differential RR cross

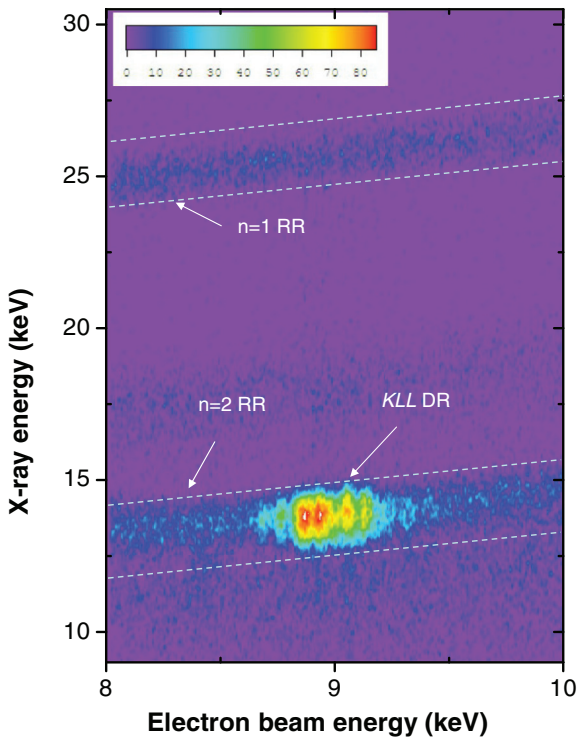

FIG. 3. (Color online) Scatter plot of x-ray intensity as functions of x-ray and electron energy.

TABLE II. Calculated dielectric capture strengths (S_{DC}) (in units of 10^{-20} cm^{2}eV) and differential resonance strengths ($\frac{dS}{d\Omega}$) (in units of 10^{-20} cm^{2}eV/sr) of hydrogenlike krypton. $|d\rangle$, $|s\rangle$, and $|f\rangle$ stand for the doubly excited, singly excited, and final states, respectively. E_r is the resonance energy in units of keV. $\mathcal{A}_d$ and $\mathcal{A}_s$ are the alignment parameter of the doubly and singly excited states, respectively. $BR^{d\to s}$ is the branching ratio for the radiative decay from the doubly to singly excited states and $BR^{s\to f}$ is the branching ratio for the decay from the singly excited to final states. W_{1st} and W_{2nd} are the angular distribution correction coefficient for the primary and secondary K x-ray emissions.

$\|d\rangle$	E_r	S_{DC}	$\mathcal{A}_d$	$\|s\rangle$	$BR^{d\to s}$	W_{1st}	$\mathcal{A}_s$	$\|f\rangle$	$BR^{s\to f}$	W_{2nd}	$\frac{dS^{1st}}{d\Omega}$	$\frac{dS^{2nd}}{d\Omega}$
$[2s^2]_0$	9.056	4.921	0	$[1s2p_{3/2}]_1$	0.090	1.00	0	$[1s^2]_0$	1	1.00	0.035	0.035
			0	$[1s2p_{1/2}]_1$	0.476	1.00	0	$[1s^2]_0$	1	1.00	0.186	0.186
$[2s2p_{1/2}]_0$	9.059	0.655	0	$[1s2s]_1$	0.956	1.00	0	$[1s^2]_0$	1	1.00	0.050	0.050
$[2s2p_{1/2}]_1$	9.070	2.083	−0.263	$[1s2s]_1$	0.837	0.95	0.132	$[1s^2]_0$	1	0.95	0.132	0.132
				$[1s2s]_0$	0.116	1.09					0.021	
$[2p_{1/2}^2]_0$	9.114	0.110	0	$[1s2p_{1/2}]_1$	0.983	1.00	0	$[1s^2]_0$	1	1.00	0.009	0.009
$[2s2p_{3/2}]_2$	9.136	1.220	−0.822	$[1s2s]_1$	0.983	1.17	−0.486	$[1s^2]_0$	1	1.17	0.112	0.112
$[2p_{1/2}2p_{3/2}]_2$	9.178	13.039	−1.042	$[1s2p_{3/2}]_1$	0.228	1.22	−0.616	$[1s^2]_0$	1	1.22	0.289	0.289
				$[1s2p_{3/2}]_2$	0.320	0.78	0.521	$[1s^2]_0$	0.897	1.16	0.259	0.346
								$[1s2s]_1\to[1s^2]_0$	0.103	0.89		0.030
				$[1s2p_{1/2}]_1$	0.366	1.22	−0.616	$[1s^2]_0$	1	1.22	0.463	0.463
$[2s2p_{3/2}]_1$	9.182	6.926	−1.380	$[1s2s]_0$	0.750	1.49					0.616	
				$[1s2s]_1$	0.108	0.76	0.690	$[1s^2]_0$	1	0.76	0.045	0.045
$[2p_{3/2}^2]_2$	9.251	10.564	−1.042	$[1s2p_{3/2}]_1$	0.552	1.22	−0.616	$[1s^2]_0$	1	1.22	0.566	0.566
				$[1s2p_{3/2}]_2$	0.377	0.78	0.521	$[1s^2]_0$	0.897	1.16	0.247	0.330
								$[1s2s]_1\to[1s^2]_0$	0.103	0.89		0.029
$[2p_{3/2}^2]_0$	9.292	0.701	0	$[1s2p_{3/2}]_1$	0.974	1.00	0	$[1s^2]_0$	1	1.00	0.054	0.054
											$\sum_{1st} = 3.08$	$\sum_{2nd} = 2.68$

sections were calculated for each charge state for the electron energies from 8 to 10 keV.

IV. RESULT AND ANALYSIS

In the data analysis, the two-dimensional plot shown in Fig. 3 was cut along the $n = 1$ and $n = 2$ RR lines, then projected onto the electron-beam energy axis to obtain the excitation functions for DR and RR, as shown in Fig. 4. In the figure, the smooth background corresponds to the $n = 1,2$ RR, whereas the sharp peaks correspond to the *KLL* DR resonances. The following formula was fitted to the experimental excitation function for the charge state $q = 33$ to 36, i.e., lithiumlike to bare ions:

$$F(E) = C(E)\sum_q f_q\left[\frac{d\sigma_{RR}(q,E)}{d\Omega} + K_q\sum_{d,f}\frac{S^q_{d\to f}W^q_{d\to f}(90^\circ)}{4\pi w\sqrt{\pi/2}}\exp\left(-2\frac{(E-E_r)^2}{w^2}\right)\right], \quad (4)$$

TABLE III. Calculated integral (S) and differential resonance strengths ($\frac{dS}{d\Omega}$) of heliumlike krypton (in units of 10^{-20} cm^{2}eV and 10^{-20} cm^{2}eV/sr). E_r and E_{hv} are the resonance energy and x-ray energy in units of keV. W is the angular distribution correction coefficient.

$\|d\rangle$	$\|f\rangle$	E_r	E_{hv}	S	W	$\frac{dS}{d\Omega}$
$[1s2s^2]_{1/2}$	$[1s^22p_{1/2}]_{1/2}$	8.821	12.859	1.743	1.00	0.139
	$[1s^22p_{3/2}]_{3/2}$		12.794	0.806	1.00	0.064
$[(1s2s)_12p_{1/2}]_{3/2}$	$[1s^22s]_{1/2}$	8.848	12.957	0.130	1.25	0.013
$[(1s2s)_02p_{1/2}]_{1/2}$	$[1s^22s]_{1/2}$	8.890	13.009	5.628	1.00	0.448
$[(1s2s)_12p_{3/2}]_{3/2}$	$[1s^22s]_{1/2}$	8.946	13.055	0.119	1.25	0.012
$[(1s2s)_12p_{3/2}]_{1/2}$	$[1s^22s]_{1/2}$	8.968	13.077	2.668	1.00	0.212
$[(1s2s)_02p_{3/2}]_{3/2}$	$[1s^22s]_{1/2}$	8.977	13.086	3.967	1.25	0.395
$[(1s2p_{1/2})_12p_{3/2}]_{5/2}$	$[1s^22p_{3/2}]_{3/2}$	8.990	12.963	10.037	1.20	0.958
$[(1s2p_{1/2})_12p_{3/2}]_{1/2}$	$[1s^22p_{1/2}]_{1/2}$	9.007	13.045	0.127	1.00	0.010
$[(1s2p_{1/2})_12p_{3/2}]_{3/2}$	$[1s^22p_{1/2}]_{1/2}$	9.013	13.051	10.005	1.25	0.995
	$[1s^22p_{3/2}]_{3/2}$		12.986	2.402	0.80	0.153
$[1s(2p_{3/2}^2)_2]_{5/2}$	$[1s^22p_{3/2}]_{3/2}$	9.058	13.031	14.092	1.20	1.346
$[1s(2p_{3/2}^2)_2]_{3/2}$	$[1s^22p_{3/2}]_{3/2}$	9.082	13.056	4.481	0.80	0.285
$[1s(2p_{3/2}^2)_0]_{1/2}$	$[1s^22p_{3/2}]_{3/2}$	9.104	13.078	1.556	1.00	0.124
						$\sum = 5.15$

TABLE IV. Same as Table III, but for lithiumlike krypton.

$\|d\rangle$	$\|f\rangle$	E_r	$E_{h\nu}$	S	W	$\frac{dS}{d\Omega}$
$[1s2s^22p_{1/2}]_1$	$[2s^2]_0$	8.954	12.926	2.05	0.79	0.129
$[(1s2s)_12p_{1/2}^2]_1$	$[2s2p_{1/2}]_0$	8.990	12.890	0.123	1.00	0.010
	$[2s2p_{1/2}]_1$		12.899	0.210	1.00	0.017
$[1s2s^22p_{3/2}]_2$	$[2p_{1/2}2p_{3/2}]_1$	9.014	12.759	0.275	1.17	0.026
	$[2p_{1/2}2p_{3/2}]_2$		12.749	0.324	0.83	0.021
	$[2p_{3/2}^2]_2$		12.689	0.111	0.83	0.007
$\{[(1s2s)_12p_{1/2}]_{1/2}2p_{3/2}\}_2$	$[2s2p_{3/2}]_2$	9.031	12.878	0.136	0.86	0.009
$[1s2s^22p_{3/2}]_1$	$[2s^2]_0$	9.037	13.009	0.442	0.91	0.032
$\{[(1s2s)_12p_{1/2}]_{3/2}2p_{3/2}\}_3$	$[2s2p_{3/2}]_2$	9.048	12.895	3.190	1.17	0.297
$[(1s2s)_02p_{1/2}^2]_0$	$[2s2p_{1/2}]_1$	9.053	12.952	0.189	1.00	0.015
$\{[(1s2s)_12p_{1/2}]_{1/2}2p_{3/2}\}_1$	$[2s2p_{1/2}]_0$	9.082	12.991	0.891	1.18	0.084
	$[2s2p_{1/2}]_1$		12.982	0.258	0.91	0.019
	$[2s2p_{3/2}]_2$		12.929	0.268	1.02	0.022
$\{[(1s2s)_12p_{1/2}]_{3/2}2p_{3/2}\}_2$	$[2s2p_{3/2}]_2$	9.092	12.938	0.794	0.87	0.055
	$[2s2p_{3/2}]_1$		12.892	0.464	1.13	0.042
$\{[(1s2s)_12p_{1/2}]_{3/2}2p_{3/2}\}_1$	$[2s2p_{1/2}]_0$	9.105	13.015	0.349	1.28	0.036
	$[2s2p_{1/2}]_1$		13.004	3.364	0.86	0.230
	$[2s2p_{3/2}]_2$		12.952	0.230	1.03	0.019
	$[2s2p_{3/2}]_1$		12.905	0.464	0.86	0.032
$\{[(1s2s)_02p_{1/2}]_{1/2}2p_{3/2}\}_1$	$[2s2p_{3/2}]_2$	9.121	12.968	0.130	1.01	0.010
$\{[(1s2s)_02p_{1/2}]_{1/2}2p_{3/2}\}_2$	$[2s2p_{1/2}]_1$	9.123	13.022	0.587	1.22	0.057
	$[2s2p_{3/2}]_2$		12.970	3.117	0.78	0.193
	$[2s2p_{3/2}]_1$		12.923	1.245	1.22	0.121
$[(1s2s)_1(2p_{3/2}^2)_2]_3$	$[2s2p_{3/2}]_2$	9.125	12.972	10.058	1.17	0.936
$[(1s2s)_1(2p_{3/2}^2)_2]_2$	$[2s2p_{3/2}]_2$	9.163	13.010	3.116	0.82	0.203
	$[2s2p_{3/2}]_1$		12.964	0.502	1.18	0.047
$[(1s2s)_1(2p_{3/2}^2)_0]_1$	$[2s2p_{3/2}]_2$	9.178	13.025	1.513	0.99	0.119
$[(1s2s)_0(2p_{3/2}^2)_2]_2$	$[2s2p_{3/2}]_2$	9.195	13.042	0.119	0.78	0.007
	$[2s2p_{3/2}]_1$		12.996	2.307	1.22	0.224
$[(1s2s)_1(2p_{3/2}^2)_2]_1$	$[2s2p_{3/2}]_1$	9.199	13.000	0.483	0.84	0.032
$[(1s2s)_0(2p_{3/2}^2)_0]_0$	$[2s2p_{3/2}]_1$	9.221	13.021	0.574	1.00	0.046
						$\sum = 3.10$

where $C(E)$ is a detecting efficiency, f_q the ion abundance for the charge state q, $d\sigma_{\rm RR}(q,E)/d\Omega$ the differential cross section of RR at 90°, $S^q_{d\to f}$ the DR resonance strength for the intermediate state d and the final state f, and $W^q_{d\to f}$ the corresponding angular correction coefficient. K_q is a factor used for correcting theoretical resonance strengths; w the width of electron-beam energy spread.

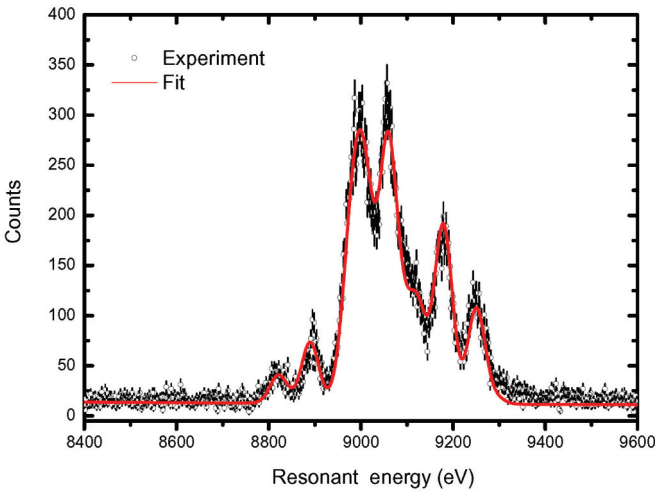

FIG. 4. (Color online) Experimental excitation function of *KLL* DR (black dot) and the theoretical resonance function fitted to the experimental data (red curve).

The present analysis is similar to that used by Knapp [7] and Yao [30]. First, the theoretical resonance strengths of hydrogenlike to lithiumlike krypton were used to obtain the ion abundance (f_q) by fitting them to the experimental excitation function. In this fitting procedure, K_q was fixed at unity for all the charge state ions. As a result, the ion abundance was obtained as listed in Table V with an electron energy width of 37 eV. Since bare krypton do not contribute to the resonant excitation function ($S^q_{d\to f} = 0$ for $q = 36$), the ion abundance of bare cannot be obtained only from the fitting procedure. The abundance ratio of bare to hydrogenlike ions was thus

TABLE V. Ion abundance f_q (%) obtained from the fitting (see text).

Parameter	Bare	H	He	Li
f_q	2.44	21.99	55.51	21.06

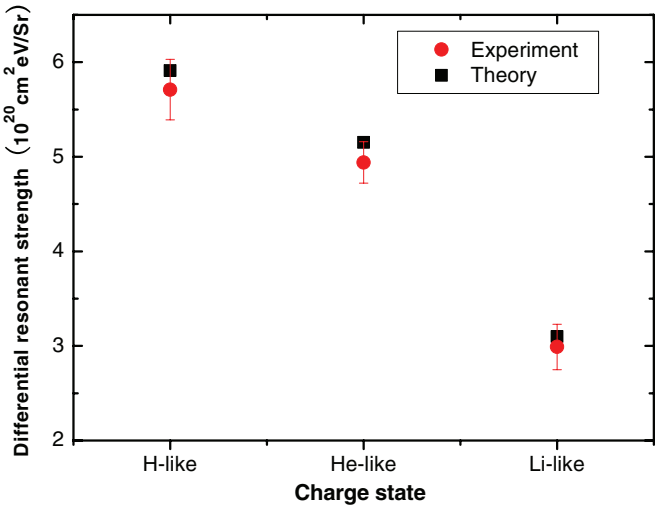

FIG. 5. (Color online) Comparison between the theory and experiment.

fixed to the value obtained from the x-ray intensity ratio for RR into $n = 1$ between hydrogenlike and bare krypton. Secondly, with fixed values of $C(E)$, f_q and w, another fitting was performed with K_q as fitting parameters. Finally, the differential resonance strengths were obtained from the fitting results of K_q. The final fitting result is shown in Fig. 4, and the experimental differential cross sections are shown in Fig. 5 and listed in Table VI with the present theoretical cross sections. Here, the differential resonance strength of hydrogenlike krypton is the sum of the contributions from both primary and secondary photon emissions. The uncertainty includes two contributions; one is the fitting error estimated in the fitting procedure weighted by the statistical uncertainty, and another is the error in the theoretical RR cross section, which was estimated to be 3% following the discussion in Ref. [7]. The comparison shows that the experimental results agree well with the theoretical calculation.

The present experimental and theoretical results are also compared with previous studies, as shown in Fig. 6. For the comparison, the integrated *KLL* resonance strength was estimated from the present experimental differential resonance strength by using the formula

$$S = \frac{4\pi}{W^*}\frac{dS}{d\Omega}, \tag{5}$$

where W^* is an effective angular distribution correction coefficient, which is defined as

$$W^* = \frac{\sum_i W_i S_i}{\sum_i S_i}. \tag{6}$$

TABLE VI. Experimental and theoretical differential resonance strengths for *KLL* DR resonance of krypton ions (in units of 10^{-20} cm^{2}eV/sr).

Ions	Experiment	Theory
H-like	5.71(32)	5.91
He-like	4.94(22)	5.15
Li-like	2.99(24)	3.10

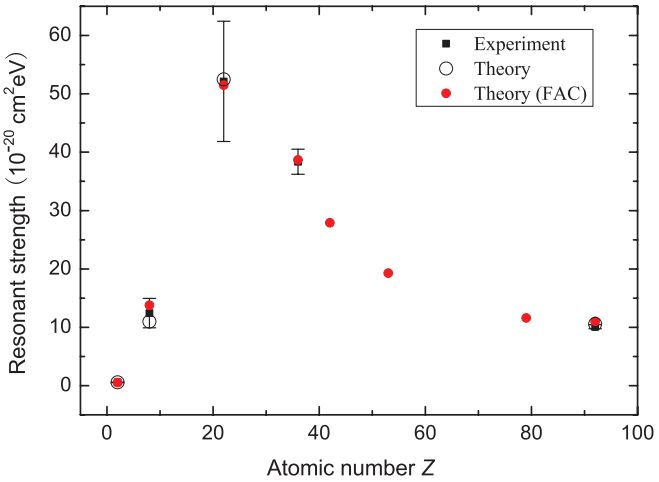

FIG. 6. (Color online) Resonance strengths for the *KLL* resonance of hydrogenlike ions. The solid red circles are the present theoretical results and the open black circles are the previous theoretical results for He^+ [31], O^{7+} [32], Ti^{22+} [15], and U^{91+} [33]. The black squares with error bars are experimental results for He^+ [34], O^{7+} [35], Ti^{22+} [15], Kr^{35+} (present), and U^{91+} [33].

Since individual resonances could not be resolved in the present experiment, the effective angular distribution correction was estimated to be 1.05 using the calculated angular distribution W_i and resonance strengths S_i for each resonance. It is noted that the resonance strengths plotted in Fig. 6 do not contain the contribution from the second decay (whereas the differential resonance strength in Fig. 5 and Table VI does). The contribution from the second decay was estimated to be 0.47 from the theoretical results listed in Table II. It is also noted that the isotropic distribution ($W^* = 1$) was assumed to obtain the integrated resonance strength for titanium from the experimental differential resonance strength [15].

As seen in the figure, the present calculated values agree well with the present and existing experimental data over the full range of atomic number. The present calculations were performed with a fully interelectron interaction operator including the Breit interaction. For the heavy element uranium ($Z = 92$), the present calculation agrees well with the previous work by Bernhardt *et al.* [33], which demonstrated significant enhancement for the absolute resonance strengths due to the Breit interaction. Due to the lack of experimental data, experiments for intermediately heavy elements are required.

V. CONCLUSIONS

We have experimentally studied the *KLL* dielectronic recombination (DR) of hydrogenlike krypton with the Tokyo electron-beam ion trap. By normalizing the DR x-ray counts to theoretical RR cross sections, the differential resonance strength has been obtained. We have also performed theoretical calculation with the flexible atomic code. The theoretical results show good agreement with the present and existing experimental data.

ACKNOWLEDGMENT

This work is supported by KAKENHI 21340111.

[1] M. J. May, S. B. Hansen, J. Scofield, M. Schneider, K. Wong, and P. Beiersdorfer, Phys. Rev. E **84**, 046402 (2011).
[2] C. Bowen and P. Kaiser, J. Quant. Spectrosc. Radiat. Transfer **81**, 85 (2003).
[3] R. E. Marrs, M. A. Levine, D. A. Knapp, and J. R. Henderson, Phys. Rev. Lett. **60**, 1715 (1988).
[4] M. A. Levine, R. E. Marrs, J. R. Henderson, D. A. Knapp, and M. B. Schneider, Phys. Scr. **T22**, 157 (1988).
[5] P. Beiersdorfer, T. W. Phillips, K. L. Wong, R. E. Marrs, and D. A. Vogel, Phys. Rev. A **46**, 3812 (1992).
[6] D. A. Knapp, R. E. Marrs, M. A. Levine, C. L. Bennett, M. H. Chen, J. R. Henderson, M. B. Schneider, and J. H. Scofield, Phys. Rev. Lett. **62**, 2104 (1989).
[7] D. A. Knapp, R. E. Marrs, M. B. Schneider, M. H. Chen, M. A. Levine, and P. Lee, Phys. Rev. A **47**, 2039 (1993).
[8] T. Fuchs, C. Biedermann, R. Radtke, E. Behar, and R. Doron, Phys. Rev. A **58**, 4518 (1998).
[9] Y. Zou, J. R. Crespo López-Urrutia, and J. Ullrich, Phys. Rev. A **67**, 042703 (2003).
[10] A. J. Gonzalez Martinez, J. R. Crespo Lopez-Urrutia, J. Braun, G. Brenner, H. Bruhns, A. Lapierre, V. Mironov, R. Soria Orts, H. Tawara, M. Trinczek, J. Ullrich, and J. H. Scofield, Phys. Rev. Lett. **94**, 203201 (2005).
[11] H. Watanabe, F. J. Currell, H. Kuramoto, Y. M. Li, S. Ohtani, B. O'Rourke, and X. M. Tong, J. Phys. B: At. Mol. Opt. Phys. **34**, 5095 (2001).
[12] B. E. O'Rourke, H. Kuramoto, Y. M. Li, S. Ohtani, X. M. Tong, H. Watanabe, and F. J. Currell, J. Phys. B: At. Mol. Opt. Phys. **37**, 2343 (2004).
[13] H. Watanabe, H. Tobiyama, A. P. Kavanagh, Y. M. Li, N. Nakamura, H. A. Sakaue, F. J. Currell, and S. Ohtani, Phys. Rev. A **75**, 012702 (2007).
[14] A. P. Kavanagh, H. Watanabe, Y. M. Li, B. E. O'Rourke, H. Tobiyama, N. Nakamura, S. McMahon, C. Yamada, S. Ohtani, and F. J. Currell, Phys. Rev. A **81**, 022712 (2010).
[15] H. Watanabe, A. P. Kavanagh, H. Kuramoto, Y. M. Li, N. Nakamura, S. Ohtani, B. O'Rourke, A. Sato, H. Tawara, X. Tong, and F. J. Currell, Nucl. Instrum. Methods Phys. Res. B: Beam Interact. Mater. Atoms **235**, 261 (2005).
[16] B. E. O'Rourke, F. J. Currell, H. Kuramoto, S. Ohtani, H. Watanabe, Y. M. Li, T. Tawara, and X. M. Tong, Phys. Rev. A **77**, 062709 (2008).
[17] D. R. DeWitt, D. Schneider, M. W. Clark, M. H. Chen, and D. Church, Phys. Rev. A **44**, 7185 (1991).
[18] N. Nakamura, J. Asada, F. J. Currell, T. Fukami, T. Hirayama, K. Motohashi, T. Nagata, E. Nojikawa, S. Ohtani, K. Okazaki, M. Sakurai, H. Shiraishi, S. Tsurubuchi, and H. Watanabe, Phys. Scr. **T73**, 362 (1997).
[19] M. F. Gu, Astrophys. J. **582**, 1241 (2003).
[20] U. Fano and J. H. Macek, Rev. Mod. Phys. **45**, 553 (1973).
[21] M. K. Inal and J. Dubau, J. Phys. B: At. Mol. Phys. **20**, 4221 (1987).
[22] M. H. Chen and J. H. Scofield, Phys. Rev. A **52**, 2057 (1995).
[23] S. Fritzsche, A. Surzhykov, and T. Stöhlker, Phys. Rev. Lett. **103**, 113001 (2009).
[24] Z. Hu, X. Han, Y. Li, D. Kato, X. Tong, and N. Nakamura, Phys. Rev. Lett. **108**, 073002 (2012).
[25] V. V. Balashov, A. N. Grum-Grzhimailo, and N. M. Kabachnik, *Polarization and Correlation Phenomena in Atomic Collisions* (Kluwer Academic/Plenum Publishers, New York, 2000).
[26] M. Aydinol, R. Hippler, I. McGrehor, and H. Kleinpoppen, J. Phys. B: At. Mol. Phys. **13**, 989 (1980).
[27] W. Jitschin, H. Kleinpoppen, R. Hippler, and H. O. Lutz, J. Phys. B: At. Mol. Phys. **12**, 4077 (1979).
[28] P. Beiersdorfer, D. A. Vogel, K. J. Reed, V. Decaux, J. H. Scofield, K. Widmann, G. Hölzer, E. Förster, O. Wehrhan, D. W. Savin, and L. Schweikhard, Phys. Rev. A **53**, 3974 (1996).
[29] R. M. Steffen and K. Alder, in *The Electromagnetic Interaction in Nuclear Spectroscopy*, edited by W. D. Hamilton (North-Holland, New York, 1975), p. 505.
[30] K. Yao, Z. Geng, J. Xiao, Y. Yang, C. Chen, Y. Fu, D. Lu, R. Hutton, and Y. Zou, Phys. Rev. A **81**, 022714 (2010).
[31] J. G. Wang, Y. Z. Qu, and J. M. Li, Phys. Rev. A **52**, 4274 (1995).
[32] M. S. Pindzola, N. R. Badnell, and D. C. Griffin, Phys. Rev. A **42**, 282 (1990).
[33] D. Bernhardt, C. Brandau, Z. Harman, C. Kozhuharov, A. Müller, W. Scheid, S. Schippers, E. W. Schmidt, D. Yu, A. N. Artemyev, I. I. Tupitsyn, S. Böhm, F. Bosch, F. J. Currell, B. Franzke, A. Gumberidze, J. Jacobi, P. H. Mokler, F. Nolden, U. Spillman, Z. Stachura, M. Steck, and T. Stöhlker, Phys. Rev. A **83**, 020701(R) (2011).
[34] D. R. DeWitt, R. Schuch, T. Quinteros, H. Gao, W. Zong, H. Danared, M. Pajek, and N. R. Badnell, Phys. Rev. A **50**, 1257 (1994).
[35] G. Kilgus, J. Berger, P. Blatt, M. Grieser, D. Habs, B. Hochadel, E. Jaeschke, D. Kramer, R. Neumann, G. Neureither, W. Ott, D. Schwalm, M. Steck, R. Stokstad, E. Szmola, A. Wolf, R. Schuch, A. Muller, and M. Wagner, Phys. Rev. Lett. **64**, 737 (1990).